Proceedings of the 21st ICSMGE, Vienna, Austria, 14 – 19 June 2026. Pistrol, Adam & Schweiger (eds.)
Published by: ÖGG, Austrian Society for Geomechanics, Salzburg, Austria, ISBN 978-3-9503898-4-5
https://doi.org/10.53243/ICSMGE2026-1458

Challenges in Morphological Characterization of Granular Materials: A Statistical Perspective

Farzad Kaviani-Hamedani, Arman Khoshghalb, Nasser Khalili, Rahim Saffari
University of New South Wales, Sydney, Australia, f.kaviani_hamedani@unsw.edu.au

Mohammad Esmailzade
Amirkabir University of Technology, Iran

ABSTRACT: Granular materials are ubiquitous in geotechnical engineering applications, including dams, backfills, and road bases. The behavior of these materials is significantly influenced by particle morphology—i.e., grain size, shape, and distribution. Accurate quantification of these attributes is therefore essential for understanding and predicting mechanical behavior. This study investigates the statistical considerations necessary for accurately quantifying the 2D morphological characteristics of irregular granular materials. Using Monte Carlo simulations, we evaluate the accuracy of derived indices used in this quantification. Three granular materials are analyzed using traditional 2D image-processing techniques. We then examine error margins in commonly used empirical equations that predict key mechanical properties (e.g., the critical state line and small-strain shear modulus) to assess the influence of sample size (Z). The findings provide practical insight into potential errors introduced when grain-scale shape descriptors are used to estimate material parameters, thereby helping researchers and practitioners improve the reliability of their analyses.

KEYWORDS: Particle Shapes; Morphology; Sample Size; Image Processing, Monte Carlo

1 INTRODUCTION

Granular materials such as sandy soils are widely used in construction and are critical to the performance of foundations. Although sands, gravels, and cobbles are among the earliest construction materials in civil engineering, predicting their mechanical properties (e.g., elastic stiffness, yield surface) and associated volumetric-change regimes remains challenging because of their inherent heterogeneity. Natural soil particles, shaped by depositional processes and mechano-chemical weathering, exhibit diverse sizes and morphologies that directly affect mechanical response.

Unlike engineered continua, the macroscopic response of granular materials is governed by microscale particle interactions—particularly particle morphology—which must be evaluated from representative samples. Morphology strongly influences mechanical behavior alongside stress state and history (Roesler, 1979; Rahhal and Lefebvre, 2000; Payan et al., 2016; Jafarian et al., 2018; Jafarian and Javdanian, 2020), relative density (Fakharian et al., 2022a; Lashkari et al., 2017; Fakharian et al., 2019, 2022b, 2023, 2024; Kaviani-Hamedani et al., 2021; Shabani and Kaviani-Hamedani, 2023; Hejazi et al., 2024; Kaviani-Hamedani et al., 2025; Hardin and Richart Jr., 1963; Hardin and Black, 1966; Hardin, 1978), drainage and loading conditions (Escribano and Nash, 2015; Wersäll et al., 2017), and soil fabric (Fakharian, Kaviani-Hamedani and Imam, 2022.; Fakharian et al., 2019, 2022b, 2023; Kaviani-Hamedani 2021; Yang et al., 2008; Bayat and Ghalandarzadeh, 2019; Shi et al., 2021).

Various thermo-hydro-mechanical characteristics of granular materials are affected by particle shape, size, gradation. There is substantial evidence for effects on mechanical properties such as shear modulus, elastic stiffness, internal friction angle, and the critical state line (Mitchell, Soga et al., 2005; Cho, Dodds and Santamarina, 2006; Peña, García-Rojo and Herrmann, 2007; Rousé, Fannin and Shuttle, 2008; Kandasami and Murthy, 2017); on elastic stiffness, yield surface, and associated volumetric behavior (Altuhafi, Coop and Georgiannou, 2016; Payan et al., 2016a, 2017; de Bono and McDowell, 2020); and on hydraulic and thermal properties—such as permeability and thermal conductivity (Lee et al., 2017; Zheng et al., 2021; He et al., 2022).

To determine the mechanical response of granular materials, various experiments have been designed to mimic in situ conditions (e.g., uniaxial, triaxial, simple shear, bidirectional simple shear, true triaxial, hollow-cylinder apparatus). These experiments have led to the development of empirical correlations (Hardin and Richart Jr., 1963; Seed and Idriss, 1970; Seed et al., 1986; Saxena and Reddy, 1989; Fioravante, 2000; Menq, 2003; Wichtmann and Triantafyllidis, 2009; Senetakis et al., 2012; Giang et al., 2017; He et al., 2019; He et al., 2022), many of which have overlooked the role of morphological characteristics. Ignoring these characteristics often reduces accuracy and necessitates conservative safety factors (Payan, 2017), owing to the limitations of grain-scale inspection and the diversity of particle sizes and shapes, which make it difficult to obtain representative, well-founded values. Therefore, explicitly addressing morphological characteristics and their diversity is essential to overcome the limitations of existing correlations.

Additionally, incorrect predictions of soil properties in foundation systems can have severe consequences. Loose, saturated sands, for instance, are prone to significant settlement and low bearing capacity and are also susceptible to liquefaction under undrained conditions (Yoshimi et al., 1989). During liquefaction, the shear strength of loose sand rapidly diminishes as the stress state approaches a critical condition, leading to sudden failure. This type of failure, known as flow liquefaction, has been responsible for several tailings-dam failures, including the Merriespruit, Mount Polley, and Fundão dams, and has sparked extensive research to uncover the contributing factors (Castro and Poulos, 1977; Lashkari et al., 2017; Fakharian and Kaviani-Hamedani, 2020; Shabani and Kaviani-Hamedani, 2023; Fakharian et al., 2024; Hejazi et al., 2024; Kaviani-Hamedani et al., 2024). Therefore, accurate morphological quantification is critically important. As with any statistical estimate, reliable values require a representative sample of sufficient size. However, the required sample size (Z) primarily depends on the variability of the target parameter and on the material's diversity in shape and size. Although numerous morphology-driven correlations exist in the literature, there is no systematic study quantifying the potential errors across different parameters.

Despite extensive advances in particle-scale characterization, there remains no systematic framework for quantifying how sampling error propagates through commonly used 2D morphological descriptors. Existing studies typically

report mean or modal values without evaluating the statistical reliability of these indices or the minimum sample size required to achieve acceptable accuracy. This gap becomes critical when morphological descriptors are used as inputs to empirical correlations for estimating stiffness, critical state friction angle, and liquefaction resistance. The present study addresses this gap by evaluating the sample-size sensitivity and associated statistical error for several widely used shape descriptors across three sands, thereby providing practitioners with guidance on the reliability of morphology-dependent correlations.

In this study, we present existing definitions of quantitative shape descriptors for three sandy soils and discuss how sample size influences the associated error for several 2D indices.

2 SHAPE DESCRIPTORS DEFINITIONS

The measurement of the 3D surface area of soil grains, as originally proposed by (Wadell, 1932), presents significant challenges. Consequently, several practical definitions of sphericity have been introduced based on a particle's projected area, essentially a 2D approximation of sphericity. The earliest definition involved calculating the ratio of the diameter of a circle with an area equal to the largest projected area of the particle to the diameter of the smallest circle that could circumscribe the particle's projection.

Table 1. Description of 2D shape descriptors.

Sphericity Parameters	Description	Parameters
S_A (Area Sphericity)	$S_A = \frac{A_s}{A_{cir}}$	A_s: area of soil particle A_{cir}: area of minimum circumscribed circle
S_D (Diameter Sphericity)	$S_D = \frac{D_c}{D_{cir}}$	D_c: diameter of a circle with the same area of soil particle D_{cir}: diameter of minimum circumscribed circle
S_C (Circle Ratio Sphericity)	$S_C = \frac{D_{ins}}{D_{cir}}$	D_{ins}: diameter of the maximum inscribed circle
S_P (Perimeter Sphericity)	$S_P = \frac{P_c}{P_s}$	P_c: perimeter of the circle with the same area of soil particle P_s: perimeter of soil particle
S_{wl}(aspect ratio)	$S_{WL} = \frac{D}{L}$	D: minimum Feret size L: maximum Feret size
R (Roundness)	$R = \frac{\sum_{i=1}^{N} R_i/N}{R_m}$	R_i is the radius of ith corner circle N: total number of corners Rm: maximum inscribed circle in the particle projection
C (Convexity)	$C = \frac{A}{A + A^*}$	A: Projected area of particle A^*: projected area of particle area when all convexities within its perimeter are filled
EL (Elongation)	$EL = \frac{D_{min}}{D_{max}}$	D_{min} and D_{max}: minimum and maximum dimension of particle

Over time, alternative sphericity definitions have been developed (Krumbein and Sloss, 1951; Santamarina and Cho, 2004; Mitchell, Soga and others, 2005; Altuhafi, O'Sullivan and Cavarretta, 2013). Table 1 summarizes commonly used 2D sphericity definitions in the literature, including those reviewed by (Mitchell, Soga and others, 2005). Table 1 also details the parameters utilized in each definition.

3 TESTED MATERIALS

This study utilizes three granular materials with irregular sizes and shapes. Their physical properties are summarized in Table 2. All materials are classified as fine to medium sand, with a significant portion of particles falling within the fine sand category. However, since sphericity is a dimensionless index, the results of this study can be generalized to grains of any size.

Figure 1 presents grain-scale SEM images of the tested sands, highlighting the varying levels of angularity across the materials. The images illustrate a notable range of angularity, from the rounded grains of Sand I to the angular grains of Sand III. These SEM images are further analysed using ImageJ software to evaluate the 2D sphericity of the particles, a process detailed in the following sections.

Table 2. Physical properties and morphological characteristics of tested materials.

Physical Properties

Soil	G_s	C_c	C_u	D_{50} [mm]	e_{max}	e_{min}
I	2.63	1.14	1.81	0.36	0.71	0.50
II	2.69	0.93	1.61	0.23	0.79	0.49
III	2.64	1.55	1.90	0.49	1.13	0.724

Morphological Characteristics

Soil	R	S_A	S_D	S_C	S_P	S_{WL}	EL	C
I	0.34	0.73	0.85	0.71	0.93	0.77	0.77	0.95
II	0.30	0.65	0.81	0.64	0.91	0.72	0.72	0.92
III	0.34	0.60	0.77	0.59	0.88	0.66	0.68	0.92

4 2D IMAGE PROCESSING

To determine the 2D sphericity of particles, several SEM images taken from tested materials (e.g., Figure 2) were assessed using Fiji which is an open-source image processing package based on ImageJ2. In this method, the sphericity and other shape descriptors can be specified as "the envelope formed by all the points of the outer surface of the particle" (e.g., (ISO, n.d.)). There are several extensive contributions in the field of 2D particle shape characterization reported in the literature (e.g., (Wadell, 1933; Yang & Luo, 2015).

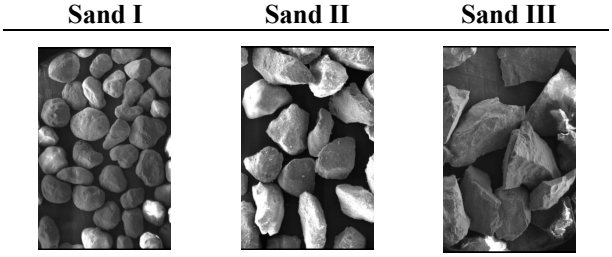

Figure 1. SEM images of tested materials.

In this study, the particles are detected using Auto Local Thresholding Methods, which is a modified local thresholding method to select the foreground from the background by boosting the threshold at lower intensities.

Figure 2(b) presents the processed SEM image shown in Figure 2 (a) after assigning the Local thresholding and filling the possible holes. This image is a binary image in which each particle's outer surface is defined by Analyze Particle module, labeling and characterizing each particle. For each material, at least 5000 particles are individually characterized (in terms of S_A, S_D, S_c, S_P, and S_{WL} as outlined in Table 2, and the sphericity is defined as the mode of the distribution curve of particle sphericity, signifying the most frequent sphericity value. Table 2 encompasses sphericity indices of irregular and semi-regular

materials. As can be seen, there is a good variety in particle sphericity indices.

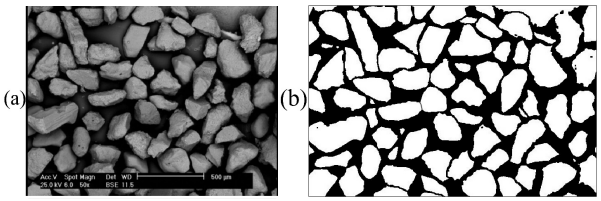

Figure 2. Typical Image Processing: (a) Raw image; (b) binarized and segmented image.

5 RESULTS

Figure 3 illustrates the distribution curves of the indices discussed in this study for the tested materials, based on over 5000 particles. The distributions show a normal pattern for all indices when the sample size is sufficiently large. Some indices, such as convexity and roundness, exhibit narrow distributions, while others, particularly S_{WL} and EL, demonstrate broader distributions, indicating greater variability in these shape descriptors.

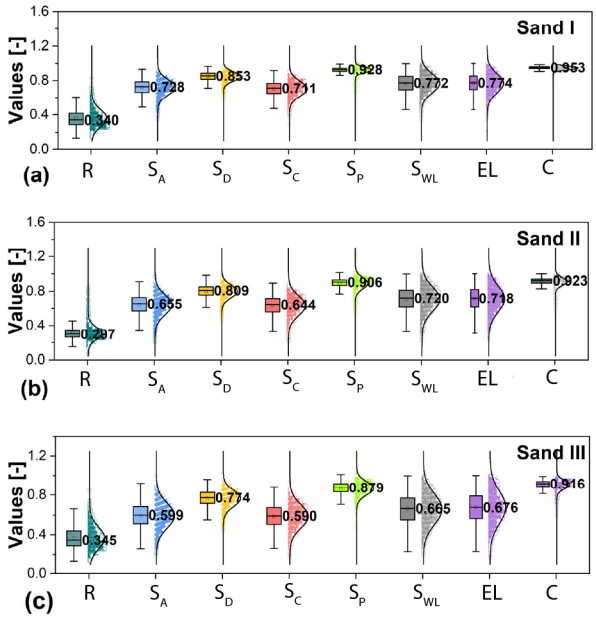

Figure 3. Distributions of morphological characteristics.

These findings suggest that the required sample size with a specific error level varies depending on the intended shape descriptor. This variability is influenced not only by the material's inherent diversity but also by the index under consideration.

To quantify the error associated with a given sample size, a Monte Carlo simulation was conducted, as illustrated in Figure 4. In this approach, one hundred random samples were drawn with the sample size ranging from 2 to 5000. The median value of each sample was calculated, and error levels were determined relative to the overall median value, which includes all particles in the soil. A total of 100 Monte Carlo iterations were selected for each sample size, which provided a stable estimate of the median and error envelope across all indices. Preliminary convergence checks showed that increasing the number of iterations beyond 100 resulted in changes of less than 1% in the estimated error levels for all descriptors. Therefore, 100 iterations offered an optimal balance between computational efficiency and statistical reliability, ensuring consistent representation of sampling variability over the full range of sample sizes.

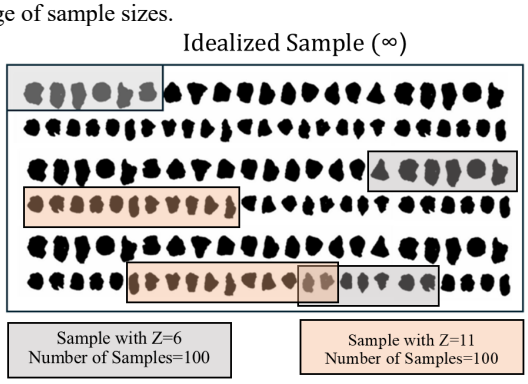

Figure 4. Monte Carlo simulations procedure.

Figure 5 illustrates the results of multiple Monte Carlo simulations performed on Soil I, covering all indices analysed in this study. Each point represents the median value of a sample of a specific size, with 100 samples evaluated per size to capture the variability. The results demonstrate that narrower distributions correspond to reduced error levels, emphasizing the link between distribution tightness and measurement accuracy.

Moreover, the error level decreases as the sample size increases, eventually converging to negligible asymptotic values. This indicates that the sample size is sufficiently large and representative, providing reliable and accurate results.

In Figure 6, the maximum error levels in S_A for different Z values across various materials. As shown, the maximum error decreases significantly with increasing sample size but remains slightly higher for materials with lower aspect ratios, particularly for flaky particles. The top projection of a flat particle tends to overestimate sphericity values and limit the visible diversity in terms of shape, as such particles typically settle on their more stable side during gravitational deposition on a plate. This bias commonly occurs during specimen preparation for most microscopic inspections.

In the literature, there are numerous empirical correlations predicting important mechanical properties such as the Critical State Line (CSL) and initial shear modulus (G_0), which work with morphological characteristics (Lashkari et al., 2020; Payan et al., 2016b, 2016a).

One of the correlations predicting the initial shear modulus based on morphological characteristics was presented by (Payan et al., 2016a) as follows:

$$G_0 = a_0 {C_u}^{a_1} (\rho)^{a_2} e^{a_3} (p'/p_a)^{C_u^{a_4}(a_5\rho + a_6)} \quad (1)$$

where, $a_0 = 84$; $a_1 = -0.14$; $a_2 = 0.68$; $a_3 = -1.29$; a_4 =0.12; a_5 =-0.23; a_6 =0.59; $\rho = (R+S)/2$; p' is the mean effective stress; e is the void ratio; C_u is the unifirmity coefficient. Moreover, as for effective friction angle at the critical state (ϕ'_{CSL}):

$$\phi'_{CSL} = 50.3 - 7.0\,R - 19.8S \quad (2)$$

Figure 7(a) and Figure 7(b) presents the developed error in G_0 and ϕ'_{CSL} due to poor sample size based on the maximum obsereved error in R and S for *soil I* when e =0.6, p' =100 kPa, respectively. As can be seen, these correlations will result in considerable error levels for sample sizes lower than 500.

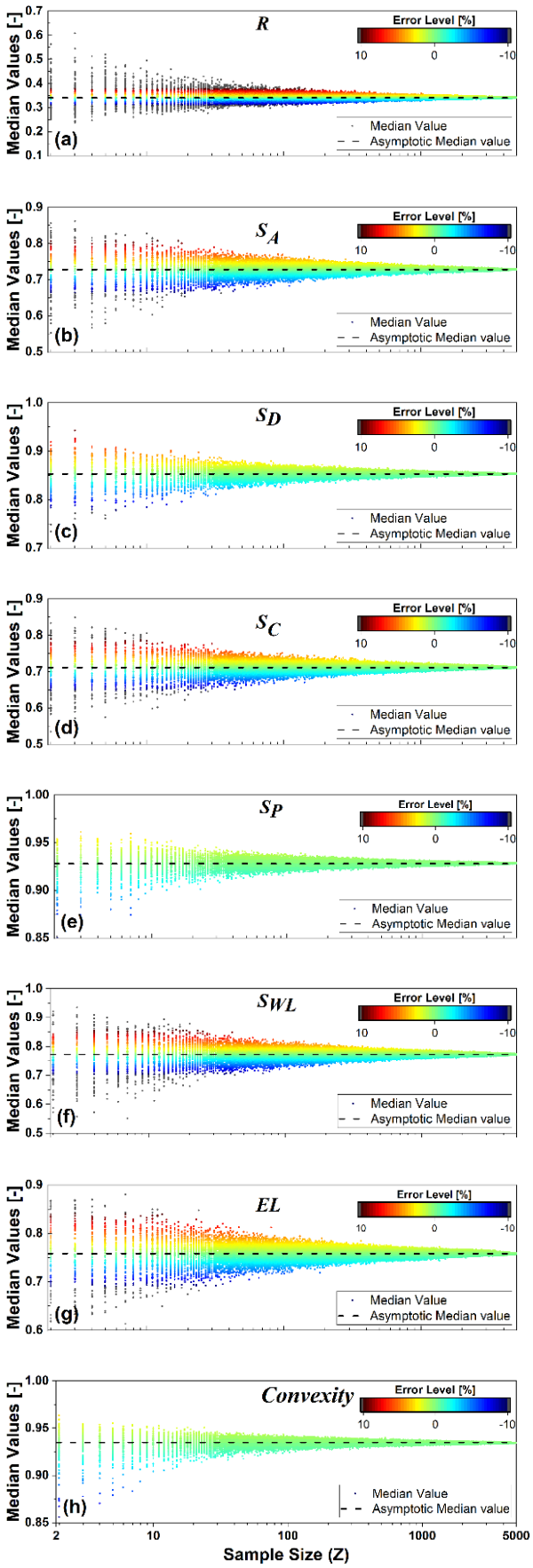

Figure 5. The results of Monte Carlo simulations for soil I: (a) R; (b) S_A; (c) S_d; (d) S_c; (e) S_p; (f) S_{wl}; (g) EL; (h) C.

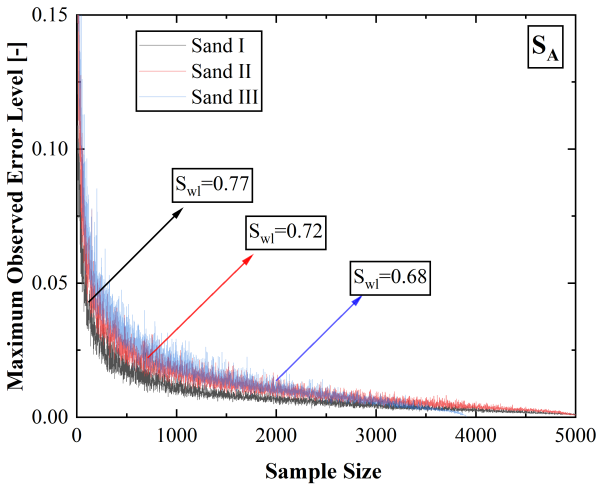

Figure 6. Maximum error levels observed for different Z.

6 PRACTICAL DISCUSSION

These findings highlight a critical consideration in the practical application of existing morphology-based correlations: their sensitivity to the quality and representativeness of the morphological input data must be considered. As demonstrated, morphological indices derived from small or statistically insufficient samples can introduce significant variability, leading to substantial prediction errors in key mechanical parameters.

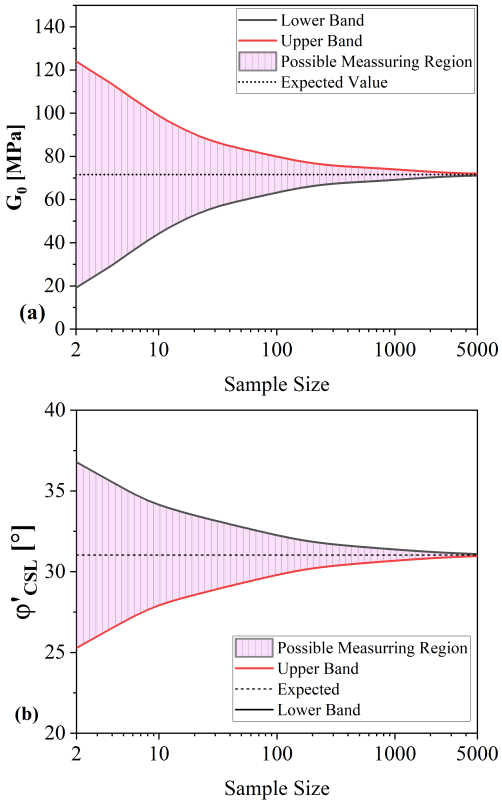

Figure 7. Errors in estimation of: (a) Shear Modulus; (b) CSL

These results demonstrate that sampling error in morphological indices can translate directly into meaningful variations in design parameters. For example, an underestimation or overestimation of sphericity or roundness by only 5–10%—a level commonly observed when fewer than 300–500 grains are analyzed—can lead to substantial deviations in predicted small-strain shear modulus or critical state friction angle. In practical

terms, this may affect assessments of settlement, stiffness degradation, cyclic resistance, and liquefaction susceptibility. In safety-critical applications such as tailings storage, embankments, and foundations on loose sands, even modest errors in morphology-based correlations may shift design outcomes across boundary conditions, effectively altering the intended safety factor. Thus, the choice of sample size is not merely a statistical consideration but also a design-reliability requirement.

7 CONCLUSIONS

This study addresses the challenges associated with quantifying various morphological characteristics of irregularly shaped granular materials using traditional 2D image processing techniques. It emphasizes the critical role of sample size in ensuring the accuracy of derived indices for such materials. The key findings are summarized as follows:

- Some indices, such as convexity and roundness, exhibit narrow distributions, while others, such as S_{WL} and EL, display broader distributions, reflecting greater variability in these shape descriptors.
- The required sample size to achieve a specific error level varies depending on the shape descriptor. This variability is influenced by both the material's intrinsic diversity and the particular index being measured.
- Regardless of the shape descriptor, the maximum error decreases as the sample size increases.

Application of existing correlations from the literature, even those developed using sufficiently large sample sizes, can yield erroneous values if the sample size is inadequate.

8 REFERENCES

Altuhafi, F., O'Sullivan, C. and Cavarretta, I., 2013. Analysis of an Image-Based Method to Quantify the Size and Shape of Sand Particles. Journal of Geotechnical and Geoenvironmental Engineering, 139(8), pp.1290–1307. https://doi.org/10.1061/(asce)gt.1943-5606.0000855.

Bayat, M. & Ghalandarzadeh, A. 2019. Influence of depositional method on dynamic properties of granular soil. International Journal of Civil Engineering, 17, 907-920.

Castro, G. and Poulos, S.J., 1977. Factors Affecting Liquefaction and Cyclic Mobility. ASCE J Geotech Eng Div, 103(6), pp.501–516. https://doi.org/10.1016/0148-9062(77)90768-9.

Cho, G.-C., Dodds, J. and Santamarina, J.C., 2006. Particle Shape Effects on Packing Density, Stiffness, and Strength: Natural and Crushed Sands. Journal of Geotechnical and Geoenvironmental Engineering, 132(5), pp.591–602. https://doi.org/10.1061/(asce)1090-0241(2006)132:5(591).

Escribano, D. & Nash, D. 2015. Changing anisotropy of G0 in Hostun sand during drained monotonic and cyclic loading. Soils and Foundations, 55, 974-984.

Fakharian, K., Hamedani, F.K., Parandian, I. and Aghdam, M.J., 2019. Investigation of fabric evolution using bidirectional shear wave velocity measurements. In: E3S Web of Conferences. EDP Sciences. https://doi.org/10.1051/e3sconf/20199203008.

Fakharian, K., Kaviani-Hamedan, F. and Imam, R., 2022a. Influences of initial anisotropy and principal stress rotation on the undrained monotonic behavior of a loose silica sand. https://doi.org/10.1139/cgj-2020-0791

Fakharian, K., Kaviani-Hamedani, F., Sooraki, A., Amindehghan, M. and Lashkari, A., 2023. Continuous bidirectional shear moduli monitoring and micro X-ray CT to evaluate fabric evolution under different stress paths. Granular Matter, [online] 25(3), p.52. https://doi.org/10.1007/s10035-023-01339-6.

Fakharian, K., Kaviani-Hamedani, F., Sooraki, A. and Mostafa, A., 2022b. A new fabric evolution monitoring method using continuous bidirectional shear wave velocity measurements in sand. In: Proceedings of the 20th International Conference on Soil Mechanics and Geotechnical Engineering. Sydney. pp.63–68. ISBN: 978-0-9946261-4-1, https://www.researchgate.net/publication/366589209_A_new_fabric_evolution_monitoring_method_using_continuous_bidirectional_shear_wave_velocity_measurements_in_sand

Fakharian, K., Hashemi, M., Kaviani-Hamedani, F., Osouli, A., Vaezian, H., Bahrami, M., Bahrami, T. and Attar, I.H., 2024. Effect of Precast Pile Driving on Liquefaction Potential Mitigation of Sandy Silts Based on CPTu. In: Proceedings of the 7th International Conference on Geotechnical and Geophysical Site Characterization. Barcelona. https://www.scipedia.com/public/Fakharian*_et_al_2024a

Fakharian, K. and Kaviani-Hamedani, F., 2020. Influence of Initial Anisotropy, Stress Path and Principal Stress Rotation on Monotonic Behavior of Clean and Mixed Sands. In: Key Engineering Materials. pp.417–430. https://doi.org/10.4028/www.scientific.net/KEM.857.417

Fioravante, V. 2000. Anisotropy of small strain stiffness of Ticino and Kenya sands from seismic wave propagation measured in triaxial testing. Soils and Foundations, 40, 129-142.

Giang, P. H. H., Van Impe, P. O., Van Impe, W. F., Menge, P. & Haegeman, W. 2017. Small-strain shear modulus of calcareous sand and its dependence on particle characteristics and gradation. Soil Dynamics and Earthquake Engineering, 100, 371-379.

Hardin, B. O. 1978. The nature of stress-strain behavior for soils. Proceedings of the ASCE Geotechnical Engineering Division Speciality Conference, 1.

Hardin, B. O. & Black, W. L. 1966. Sand stiffness under various triaxial stresses. Journal of the Soil Mechanics and Foundations Division, 92, 27-42.

Hardin, B. O. & Richart Jr, F. E. 1963. Elastic wave velocities in granular soils. Journal of the Soil Mechanics and Foundations Division, 89, 33-65.

He, H., Li, W. & Senetakis, K. 2019. Small strain dynamic behavior of two types of carbonate sands. Soils and Foundations, 59, 571-585.

He, S. H., Goudarzy, M., Ding, Z., Sun, Y., Xu, T. & Zhang, Q. F. 2022. Small-strain shear modulus (Gmax) and microscopic pore structure of calcareous sand with different grain size distributions. Granular Matter, 24, 112.

Hejazi, M., Fakharian, K. and Kaviani-Hamedani, F., 2024. Permanent deformation and particle crushability of calcareous sands under cyclic traffic-induced loadings through simple shear apparatus. Transportation Geotechnics, 49, p.101428. https://doi.org/https://doi.org/10.1016/j.trgeo.2024.101428.

ISO, D.I.N., n.d. ISO 9276-6:2008 Representation of Results of Particle Size Analysis—Part 1: Graphical Representation, 1st.

Jafarian, Y. & Javdanian, H. 2020. Small-strain dynamic properties of siliceous-carbonate sand under stress anisotropy. Soil Dynamics and Earthquake Engineering, 131, 106045.

Jafarian, Y., Javdanian, H. & Haddad, A. 2018. Dynamic properties of calcareous and siliceous sands under isotropic and anisotropic stress conditions. Soils and Foundations, 58, 172-184.

Kandasami, R.K. and Murthy, T.G., 2017. Manifestation of particle morphology on the mechanical behaviour of granular ensembles Manifestation of particle morphology on the mechanical. Granular Matter, (February). https://doi.org/10.1007/s10035-017-0703-z.

Kaviani-Hamedani, F., Fakharian, K. and Lashkari, A., 2021. Bidirectional Shear Wave Velocity Measurements to Track Fabric Anisotropy Evolution of a Crushed Silica Sand during Shearing. Journal of Geotechnical and Geoenvironmental Engineering, 147(10). https://doi.org/10.1061/(asce)gt.1943-5606.0002622.

Kaviani-Hamedani, F., Fakharian, K., Shabani, F., Khoshghalb, A., Shirkavand, D. and Baghbani, A., 2025. On the effects of multi-directional initial anisotropy on the monotonic constant volume response of a silica sand. Canadian Geotechnical Journal, [online] 62, pp.1–23. https://doi.org/10.1139/cgj-2024-0248.

Kaviani-Hamedani, F., Fakharian, K., Shirkavand, D., Khoshghalb, A., Shabani, F., Sooraki, A. and Rezaie, A., 2024. Exploring the Effects of Initial Fabric Anisotropy Due to Pre-shearing Stress History in Different Directions on the Undrained Behaviour of Loose Sands. International Journal of Geomechanics. https://doi.org/10.1061/IJGNAI/GMENG-9574.

Krumbein, W.C. and Sloss, L.L., 1951. Stratigraphy and sedimentation. LWW.

Lashkari, A., Falsafizadeh, S.R., Shourijeh, P.T. and Alipour, M.J., 2020. Instability of loose sand in constant volume direct simple

shear tests in relation to particle shape. Acta Geotechnica, 15(9), pp.2507–2527. https://doi.org/10.1007/s11440-019-00909-4.
Lashkari, A., Karimi, A., Fakharian, K. and Kaviani-Hamedani, F., 2017. Prediction of undrained behavior of isotropically and anisotropically consolidated firoozkuh sand: Instability and flow liquefaction. International Journal of Geomechanics, 17(10), pp.1–17.https://doi.org/10.1061/(ASCE)GM.1943-622.0000958.
Menq, F. Y. 2003. Dynamic Properties of Sandy and Gravelly Soils, The University of Texas at Austin.
Mitchell, J.K., Soga, K. and others, 2005. Fundamentals of soil behavior. John Wiley \& Sons New York. https://doi.org/10.1680/geot.2008.58.3.227.
Payan, M., Khoshghalb, A., Senetakis, K. and Khalili, N., 2016a. Effect of particle shape and validity of Gmax models for sand: A critical review and a new expression. Computers and Geotechnics, 72, pp.28–41. https://doi.org/10.1016/j.compgeo.2015.11.003.
Payan, M., Khoshghalb, A., Senetakis, K. and Khalili, N., 2016b. Small-strain stiffness of sand subjected to stress anisotropy. Soil Dynamics and Earthquake Engineering, 88, pp.143–151. https://doi.org/https://doi.org/10.1016/j.soildyn.2016.06.004.
Payan, M. 2017. Study of Small Strain Dynamic Properties of Sands and Silty Sands, The University of New South Wales, Sydney, Australia.
Peña, A.A., García-Rojo, R. and Herrmann, H.J., 2007. Influence of particle shape on sheared dense granular media. Granular Matter, 9(3), pp.279–291. https://doi.org/10.1007/s10035-007-0038-2.
Rahhal, M. & Lefebvre, G. 2000. Understanding the effect of a static driving shear stress on the liquefaction resistance of medium dense granular soils. Soil Dynamics and Earthquake Engineering, 20, 397-404.
Roesler, S. K. 1979. Anisotropic shear modulus due to stress anisotropy. Journal of the Geotechnical Engineering Division, 105, 871-880.
Rousé, P.C., Fannin, R.J. and Shuttle, D.A., 2008. Influence of roundness on the void ratio and strength of uniform sand. Géotechnique, 58(3), pp.227–231. https://doi.org/10.1680/geot.2008.58.3.227.
Santamarina, J.C. and Cho, G.C., 2004. Soil behaviour: The role of particle shape. Advances in Geotechnical Engineering: The Skempton Conference - Proceedings of a Three Day Conference on Advances in Geotechnical Engineering, organised by the Institution of Civil Engineers, pp.604–617.
Saxena, S. K. & Reddy, K. R. 1989. Dynamic Moduli and Damping Ratios for Monterey No. 0 Sand by Resonant Column Tests. Soils and Foundations, 29, 37-51.
Seed, H. B. & Idriss, I. 1970. Soil moduli and damping factors for dynamic response analyses. EERC 70-10. Earthquake Engineering Research Centre, University of California, Berkeley, Calif, United States of America.
Seed, H. B., Wong, R. T., Idriss, I. & Tokimatsu, K. 1986. Moduli and damping factors for dynamic analyses of cohesionless soils. Journal of Geotechnical Engineering, 112, 1016-1032.
Senetakis, K., Anastasiadis, A. & Pitilakis, K. 2012. The small-strain shear modulus and damping ratio of quartz and volcanic sands. Geotechnical Testing Journal, 35.
Shabani, F. and Kaviani-Hamedani, F., 2023. Cyclic response of sandy subsoil layer under traffic-induced principal stress rotations: Application of bidirectional simple shear apparatus. Soil Dynamics and Earthquake Engineering.
Shi, J., Haegeman, W. & Cnudde, V. 2021. Anisotropic small-strain stiffness of calcareous sand affected by sample preparation, particle characteristic and gradation. Géotechnique, 71, 305-319.
Wadell, H., 1932. Volume, Shape, and Roundness of Rock Particles. The Journal of Geology, 40(5), pp.443–451.
Wadell, H., 1933. Sphericity and Roundness of Rock Particles. 41(3), pp.310–331.
Yang, J. and Luo, X.D., 2015. Exploring the relationship between critical state and particle shape for granular materials. Journal of the Mechanics and Physics of Solids, 84, pp.196–213. https://doi.org/10.1016/j.jmps.2015.08.001.
Wersäll, C., Nordfelt, I. & Larsson, S. 2017. Soil compaction by vibratory roller with variable frequency. Géotechnique, 67, 272-278.
Wichtmann, T. & Triantafyllidis, T. 2009. Influence of the grain-size distribution curve of quartz sand on the small strain shear modulus Gmax. Journal of Geotechnical and Geoenvironmental Engineering, 135, 1404-1418.
Yang, Z., Li, X. & Yang, J. 2008. Quantifying and modelling fabric anisotropy of granular soils. Géotechnique, 58, 237-248.
Yoshimi, Y., Tokimatsu, K. & Hosaka, Y. 1989. Evaluation of liquefaction resistance of clean sands based on high-quality undisturbed samples. Soils and Foundations, 29, 93-104.